

A novel steady-state visually evoked potential-based brain-computer interfaces using trans-subject feature fusion approach

Manjula Krishnappa¹, Madaveeranahally B. Anandaraju²

¹Department of Electronics and Communication, S J C Institute of Technology, Chikkaballapur, India

²Department of Electronics and Communication, B G S Institute of Technology, Mandya, India

Article Info

Article history:

Received Dec 18, 2023

Revised May 15, 2024

Accepted Jun 5, 2024

Keywords:

Brain activity

BCI

Electroencephalogram

SSVEP

TFA

ABSTRACT

A brain-computer interface (BCI) is a transformative technology that enables users to control external devices or communicate solely through the analysis of their brain activity. One promising aspect of BCIs is the utilization of steady-state visually evoked potentials (SSVEPs), a neurophysiological response in the brain that synchronizes with repetitive visual stimuli. This paper introduces a novel approach known as the trans-subject feature fusion approach (TFA), designed to improve SSVEP-based BCIs. This methodology streamlines data pre-processing, creates invariant SSVEP templates, and simplifies calibration, addressing key challenges that have hindered BCI adoption. By doing so, the main aim is to contribute to the advancement of BCIs, making them more accessible and efficient for a range of applications, from assistive technologies to healthcare, ultimately enhancing users' communication, and control capabilities.

This is an open access article under the [CC BY-SA](https://creativecommons.org/licenses/by-sa/4.0/) license.



Corresponding Author:

Manjula Krishnappa

Department of Electronics and Communication, S J C Institute of Technology

Chikkaballapur, Karnataka, India

Email: manjula_22k@rediffmail.com

1. INTRODUCTION

The utilization of a brain-computer interface (BCI) enables the control of a device exclusively through the analysis of an individual's brain activity. The integration of hardware and software components enables the facilitation of communication between the user and the device [1]. Electroencephalogram (EEG)-based BCI systems are frequently employed in BCI research due to their convenient setup, non-intrusive nature, and portability. Significant progress has been made in the field of BCIs utilizing steady-state visually evoked potentials (SSVEPs) over the past decade, as evidenced by a comprehensive review SSVEPs refer to neurophysiological responses observed in the brain that exhibit synchronization with the frequency of recurring and periodic visual stimuli [2]. The occipital region is responsible for registering significant cognitive responses when an individual directs their gaze towards an object that is flashing at a specific frequency, along with its corresponding harmonics. The SSVEP BCI utilizes the allocation of a specific frequency of presentation to each target to facilitate the provision of multiple targets, with each target corresponding to a command [3]. When an individual directs their visual attention towards a specific target, it becomes possible to analyze their EEG signals to identify the characteristics associated with that target.

SSVEP BCIs are remarkable due to their notable information transfer rates (ITRs), minimal user training prerequisites, and the absence of individual decoder calibration [4]. The SSVEP responses may be affected by different visual stimulus characteristics, such as size, color, contrast, inter-stimulus distance, frequency, and the type of stimulator used, such as light-emitting diodes (LEDs) or computer screens. Currently, the field of study is marked by a limited availability of commercial or clinical systems.

Most speller systems commonly employ neurophysiological protocols, such as SSVEPs, event-related desynchronization/synchronization (ERD/ERS), and event-related potentials like P300 [5]. Previous studies have indicated that the SSVEP pattern demonstrates higher performance in accurate categorization compared to other EEG signal patterns. Furthermore, ongoing research is currently being conducted on BCI devices that make use of SSVEP. The main aim of this research is to explore the practical applications of these devices. The SSVEP speller employs a graphic user interface (GUI) to generate specific EEG patterns in response to a designated stimulus. The visual stimuli utilized in this system exhibit distinct positive and negative fluctuations [6]. To ensure an accurate representation of the relevant character, the user should focus their attention on the specified stimulus. This approach offers the advantage of decreasing the amount of training time needed for model calibration [7]. Furthermore, there has been a notable increase in the number of stimuli utilized to enhance the efficiency of the BCI speller. The implementation of a GUI is widely acknowledged as a crucial factor in enhancing performance in this domain. The Bremen speller is widely acknowledged as one of the earliest high-speed SSVEP BCI spellers that were developed using the multi-target stimulus paradigm.

In recent years, there has been an increasing focus among researchers on BCI spellers, also known as alphabetic BCI systems [8]-[10]. The three EEG signals commonly employed for spelling tasks include the sensorimotor rhythm (SMR), P300 event-related potential (ERP), and SSVEP. The SSVEP refers to a neurophysiological occurrence that involves a regular neural reaction triggered by a repetitive visual stimulus [11]. The response is accurately positioned within the central visual field of the subject. The SSVEP speller is widely acknowledged as a highly promising paradigm for real-world BCI applications. The primary reason for this is the notable attributes of the system, which include a high ITR, easy deployment, and minimal user training time requirement [12]-[14].

The BCI speller continues to be a prominent area of investigation in various research studies, along with other applications of BCI technology such as communication and external device control. SSVEP-based BCI spellers provide numerous benefits when compared to alternative control signals/modalities in BCI systems [15]-[18]. The benefits of this approach encompass enhanced ITR, increased signal-to-noise ratio, decreased number of necessary EEG channels, and reduced training durations. Hierarchical structures have been extensively employed in spellers that depend on SSVEP. BCIs offer numerous advantages in improving the effectiveness of logical or intuitive tasks. The development of the brain painting (BP) application for the P300 BCI incorporated the fundamental principle of user-centered design [19]-[22]. The primary objective of the BP application is to address the fundamental human requirement for enhanced communication. This is achieved by analyzing the preferences of end-users, including individuals who have been diagnosed with amyotrophic lateral sclerosis (ALS). The application is designed to cater to these preferences, even when utilizing an “alternative communication channel”. The utilization of an alternate channel in this specific scenario enabled the formation of unique visual representations, leading to an innovative design for the BCI [23].

The motivation behind this is the transformative potential of BCIs and the persistent challenges that hinder their widespread adoption. These challenges include time-consuming calibration, limited ITRs, and the need for extensive user training. To address these issues, we focus on leveraging SSVEPs to enhance BCI efficiency and usability. Our research aims to develop an optimized BCI system that reduces calibration time, improves accuracy, and simplifies the user experience. By doing so, we aspire to contribute to the advancement of BCIs, making them more accessible and efficient for various applications, including assistive technology and healthcare. Ultimately, our motivation lies in empowering individuals with enhanced communication and control capabilities through SSVEP-based BCIs, thereby improving their quality of life.

- A novel approach is known as the trans-subject feature fusion approach (TFA) for improved SSVEP-based BCI detection.
- Invariant templates: this research introduces invariant templates for SSVEP-based BCIs, which are robust to variations in user responses, enhancing SSVEP detection accuracy.

2. PROPOSED METHOD

The proposed methodology for SSVEP-based BCIs consists of several key steps. It begins with data pre-processing, where visual latency and power noise are removed, and relevant data is extracted using filters. Subsequently, spatial filters and SSVEP templates are designed, involving the calibration data from a single source and the transfer of common knowledge across subjects to construct internally and mutually invariant templates. The SSVEP data is divided into trial data for the target and multi-trial data to train templates. The training process involves internal and mutual variant spatial filter creation. Then, in the testing phase, spatial filters are tested and evaluated. SSVEP detection is performed, and the target stimulus frequency is determined. Finally, a decomposition step involves calculating sub-band information. The workflow aims to optimize SSVEP-based BCIs, making them more efficient and user-friendly.

2.1. Data pre-processing

The visual latency, the first data is removed from the SSVEP signal analysis, and the data is extracted via the filtered order and band. A filter notch at 50 Hz is used to discard the power-noise. The data prepared is completed, and the data processing and the target are detected and then performed.

2.2. Spatial filters and SSVEP template

The individual calibration data from a single source is subjected to corresponding $p - th$ stimulus and is depicted as $Z_p = [Z_p^1, Z_p^2, \dots, Z_p^{P_d}] \in T^{P_e * P_f * P_d}$, and $p = 1, 2, \dots, P_h$. However, P_e, P_f, P_d , and P_h denotes the channels for the sampling point, including the blocks and the number of stimuli. $Z_p^d \in T^{P_e * P_f}$ ($d = 1, 2, \dots, P_d$) depicts the $d - th$ block of data for Z_p . The common knowledge is transferred across various subjects for transferring, to construct internal and mutually invariant templates within a trial-test measure by spatial filter using SSVEP data through different blocks. The separated EEG data Z_p is distinguished into two parts according to each block d . The trial data Z_p^d transferred from block d and multi-trial data as δ_p^d is transferred for template training denoted as mentioned in (1).

$$\delta_p^d = [Z_p^1, \dots, Z_p^{d-1}, Z_p^{d+1}, \dots, Z_p^{P_d}] \quad (1)$$

SSVEPs from the neighboring –location stimulus share a similar spatial pattern that contains similar frequency information. The neighboring stimulus data is used to transfer the trained template. The neighbor of the $p - th$ stimulus to adjust horizontal and vertical stimuli is shown as $p^1 - th, p^2 - th, \dots, p^{P_j} - th$ stimuli. The collection of neighbors for $p - th$ stimulus is depicted in (2). $Z_{p_j} \in T^{P_e * P_f * P_d}$ ($j = 1, 2, \dots, P_j$) is the SSVEP data consisting of the neighboring stimuli, j is the index of the neighbor for the $p - th$ stimulus, and along with this the neighboring stimuli P_j . Simultaneously with $\delta_p^d \in T^{P_e * P_f * P_{(d-1)}}$ represented as in (3).

$$\vartheta_p = \{Z_{p^1}, Z_{p^2}, \dots, Z_{p^{P_j}}\}, \quad (2)$$

$$\delta_{p_j}^d = [Z_{p_j}^1, \dots, Z_{p_j}^{d-1}, Z_{p_j}^{d+1}, \dots, Z_{p_j}^{P_d}] \quad (3)$$

The $d - th$ combination of SSVEP data consisting of the target along with the neighboring stimuli data. Z_p^d, δ_p^d and $\delta_{p_j}^d$ ($h = 1, 2, \dots, P_j$). Whereas d is in the range of 1 to P_d for each stimulus p , there are P_d variations for the SSVEP training data. The $d - th$ variation for the SSVEP training data the training method involves the transferred spatial features that consist of three steps. Algorithm 1 shows the proposed workflow algorithm.

- The internal variant of the spatial filter and the template for each subject source extract the frequency information across the neighboring stimulus.
- Calculation of the mutually invariant spatial filter and the template from various sources subjected to understanding the common knowledge across shared subjects.
- While training a test-trial spatial filter data by incorporation of internal and mutual invariant samples.

Algorithm 1. Of the proposed workflow

```

Input Initialize  $P_e, P_f, P_d, P_j, o, P_1, P_h$ 
Step 1 Training Phase
  for d in range (1,  $P_d + 1$ ):
    for o in range (0):
      Internal invariant template
      for q in range (1,  $P_h + 1$ ):
        Calculate  $Y(o, q, d), V(o, q, d)$ 
Step 2 Mutually invariant template
  for o1 in range (0):
    for o2 in range (0):
      if 1 != o2:
        Calculate E12, E21, E11, E22
  for p in range (1,  $P_h + 1$ ):
    Calculate  $X(p, d)$  using the optimization problem (eq. 12)
    Calculate  $Y(o, q)$  and  $V(o, q)$  by averaging across  $P_d$ 
Step 3 Testing Phase
  for o in range (0):
    for q in range (1,  $P_h + 1$ ):

```

```

        Calculate  $W(o, q)$  using the test-trial spatial filter (eq. 16)
Step 4 SSVEP Detection
    for p in range (1,  $P_h + 1$ ):
        for o in range ( $O$ ):
            Calculate  $[\mu_p(1)][\mu_p(2)][\mu_p(3)][\mu_p(4)$ 
            Calculate  $\varphi_p$  (eq. 24)
Step 5 Decomposition
    for p in range (1,  $P_h + 1$ ):
        for l in range (1,  $P_l + 1$ ):
            Calculate  $\tau(p, l)$  for each sub-band
            Calculate  $\gamma(p)$ 
            Determine the target frequency with the maximum correlation
             $target\_stimulus = np.argmax(\varphi)$ 
Output Output the detected target stimulus (SSVEP frequency)
    
```

2.2.1. Internal invariant template

This is obtained for each source subject depicted as o . The corresponding spatial filter to the $p - th$ stimulus $y_{o,q}^d \in T^{P_e}$ is evaluated by maximizing the subjective correlation through corresponding SSVEPs corresponding to the target and the neighboring stimuli $\delta_{o,q}^d \in T^{P_e * P_f * P(d-1)}$ and $\delta_{o,q^j}^d \in T^{P_e * P_f * P(d-1)}$ ($j = 1, 2, \dots, P_j$) through each subject o . Upon simplification of the expression $\delta_{o,q}^d$ and δ_{o,q^j}^d defined by (1) and (3) to define the multi-trial data as given in (4). $\delta_{o,q}^{d_m} \in T^{P_e * P_f}$ ($m = 1, 2, \dots, P_v$). P_v is the number of trials for the multi-trial data and $P_v = P_d - 1$, in a similar way as given in (5). The invariant spatial filter $y_{o,q}^d$ is evaluated as given in (6).

$$\delta_{o,q}^d = [\delta_{o,q}^{d1}, \delta_{o,q}^{d2}, \dots, \delta_{o,q}^{dP_v}] \tag{4}$$

$$\delta_{o,q^j}^d = [\delta_{o,q^j}^{d1}, \delta_{o,q^j}^{d2}, \dots, \delta_{o,q^j}^{dP_v}] \tag{5}$$

$$y_{o,q}^d = \frac{argmax_y U_y}{y^V S_y} \tag{6}$$

$$U = cov(\delta_{o,q}^d) + \sum_{j=1}^{P_j} cov(\delta_{o,q^j}^d) \tag{7}$$

$$\delta_{o,q}^d = \frac{1}{P_v} \sum_{v=1}^{P_v} \delta_{o,q}^{d_m}, \tag{8}$$

$$\delta_{o,q^j}^d = \frac{1}{P_v} \sum_{v=1}^{P_v} \delta_{o,q^j}^{d_m} \tag{9}$$

Wherein, the result of the co-variances for the trial data obtained from $p - th$ stimulus with its neighboring stimulus is shown as in (10). The decomposition of $S^{-1} U$ solved by (6), the spatial filter $y_{o,q}^d$ is evaluated by the eigenvector corresponding to the eigenvalue. The spatial filter $y_{o,q}^d$ and the invariant template $V_{o,q}^d \in T^{P_f}$ for the relevant source subjected as o obtained via as mentioned in (11).

$$S = \sum_{v=1}^{P_v} cov(\delta_{o,q}^{d_m}) + \sum_{j=1}^{P_j} \sum_{m=1}^{P_v} cov(\delta_{o,q^j}^{d_m}) \tag{10}$$

$$V_{o,q}^d = y_{o,q}^d V_{\delta_{o,q}^d}^d \tag{11}$$

3. PERFORMANCE EVALUATION

The deep neural network (DNN) is evaluated through the utilization of the dataset, specifically, the Benchmark [24] A thorough experimental analysis is carried out in comparison of the results with state-of-the-art approaches that have been previously evaluated on specific datasets and have demonstrated favorable outcomes. The following methods are used for comparison the state-of-art techniques used are convolutional correlation analysis (Conv-CA), ms-eTRCA, ensemble-task-related component analysis (eTRCA), two stage-correlated component analysis (TSCORRCA), modified extended-canonical correlation analysis (m-extended-CCA), extended-canonical correlation analysis (extended-CCA), and two stage-correlated component analysis (CORRCA). The test methodologies utilized for each of these methods are consistently

maintained in the comparisons. To optimize the patient's periods of rest, a BCI SSVEP speller experiment consists of several blocks. The Benchmark dataset is composed of six blocks. In our performance evaluations, we utilize a leave-one-block-out approach to facilitate comparisons. Our model is trained on a specific subset of either 5 or 3 blocks, and its performance is then evaluated on the remaining block. The mean classification accuracy and ITR, along with their respective standard errors, are presented for each signal length T within the range of $T=0.2, 0.3, 1.0$. During the calculation of the index of task performance (ITR), a gaze shift time of 0.5 seconds is factored in. The testing is performed utilizing a predetermined set of nine channels, specifically Pz, PO3, PO5, PO4, PO6, POz, O1, Oz, and O2. In addition, comprehensive testing is conducted using all 64 available channels to thoroughly showcase the efficacy of our DNN. The utilization of 64 channels offers numerous advantages when compared to the pre-determined selection. Additionally, an analysis is conducted to evaluate the impact of the number of sub-bands and channels on the efficacy of identification.

3.1. Dataset details

The BCI SSVEP speller trials are evaluated on the Benchmark dataset. This features 35 healthy participants, six sessions with a 5×8 -character matrix flashing 40 characters at frequencies from 8 to 15.8 Hz. EEG data was collected from 64 channels.

3.1.1. Benchmark dataset

A cohort of 35 participants, all in a state of good health, were chosen to participate in the BCI SSVEP speller trials. Throughout these trials, data was systematically collected and meticulously recorded to establish a comprehensive reference dataset. Each experiment is composed of six blocks, which are also referred to as sessions. During the execution of the program, a matrix of size 5 by 8 is displayed on the screen. The matrix consists of a group of 40 specific characters that exhibit flashing patterns at different frequencies. The frequency range spans from 8 to 15.8 Hz, with a uniform increment of 0.2 Hz. A minimum phase difference of 0.5 is guaranteed to be maintained between consecutive frequencies. The acquisition of EEG data employs a comprehensive set comprising 64 channels. A block comprises 40 trials, where each trial represents a target character. The trials are presented in a randomized sequence. The trial is initiated by displaying a visual stimulus on the screen for a precise duration of 0.5 seconds. The primary objective of this is to effectively guide the subject's visual attention towards the intended target. Following this, a stimulation period of 5 seconds occurs, which is then followed by an offset of 0.5 seconds. The EEG signal undergoes down-sampling, resulting in a reduction of its frequency to 250 Hz. Based on the dataset, the average visual delay observed among the individuals is approximately 140 ms. Figure 1 shows the character matrix layout for the stimulus presentation in the experiments of the Benchmark dataset.

>>	8.0Hz 0	9.0Hz 0.5 π	10.0Hz π	11.0Hz 1.5 π	12.0Hz 0	13.0Hz 0.5 π	14.0Hz π	15.0Hz 1.5 π
8.2Hz 0.5 π	9.2Hz π	10.2Hz 1.5 π	11.2Hz 0	12.2Hz 0.5 π	13.2Hz π	14.2Hz 1.5 π	15.2Hz 0	
8.4Hz π	9.4Hz 1.5 π	10.4Hz 0	11.4Hz 0.5 π	12.4Hz π	13.4Hz 1.5 π	14.4Hz 0	15.4Hz 0.5 π	
8.6Hz 1.5 π	9.6Hz 0	10.6Hz 0.5 π	11.6Hz π	12.6Hz 1.5 π	13.6Hz 0	14.6Hz 0.5 π	15.6Hz π	
8.8Hz 0	9.8Hz 0.5 π	10.8Hz π	11.8Hz 1.5 π	12.8Hz 0	13.8Hz 0.5 π	14.8Hz π	15.8Hz 1.5 π	

Figure 1. The character matrix layout for the stimulus presentation in the experiments of the Benchmark dataset

3.1.2. Results for Benchmark dataset

In Figure 2 the accuracy graph is plotted for the Benchmark dataset across 9 channels, the comparison of various methods, including CORRCA, extended-CCA, m-extended-CCA, TSCORRCA, eTRCA, ms-eTRCA, Conv-CCA, existing, and proposed system (PS), reveals that PS consistently

outperforms the other methods. PS achieves the highest values of signal strength in all channels, indicating higher performance. At channel 0.2, PS scores 60.5, surpassing existing system (ES) at 58 and demonstrating its advantage. This trend continues across all channels, with PS consistently delivering the highest signal strength values. At channel 0.8, PS scores an impressive 95.2, and ES [25] exhibits 92.6. These results highlight PS as the best performer in terms of signal strength across the 9 channels.

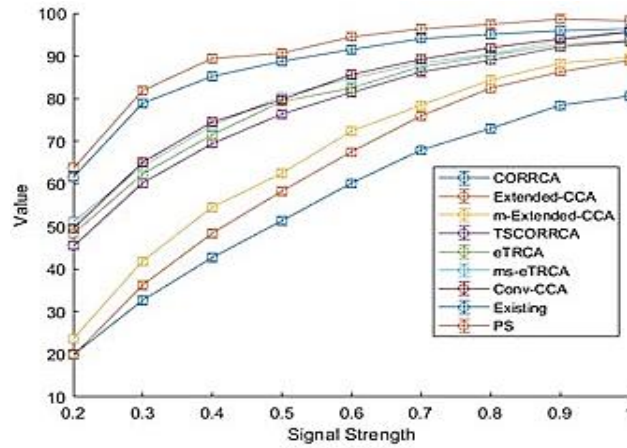


Figure 2. Accuracy graph of 9 channels for Benchmark dataset comparison

The Figure 3 analysis of performance across 64 channels, reveals that PS consistently outperforms the other methods. PS achieves the highest values of signal strength in all channels, indicating higher performance. At channel 0.2, PS scores 63.8, surpassing ES [22] at 61.59 and demonstrating its advantage. This continues across all channels, with PS consistently delivering the highest signal strength values. At channel 0.8, PS depicts a value of 97.4, ES showcases 95.78. These results highlight PS as the best performer in terms of signal strength across the 64 channels.

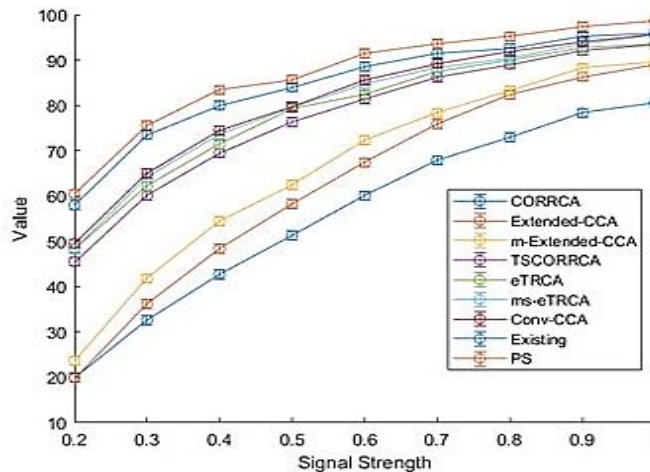


Figure 3. Accuracy graph of 64 channels for Benchmark dataset comparison

Figure 4 the analysis of performance across 9 channels concerning image transmission rate (ITR), the comparison of various methods, including CORRCA, Extended-CCA, m-Extended-CCA, TSCORRCA, eTRCA, ms-eTRCA, Conv-CCA, existing, and PS, indicates that PS consistently outperforms the other methods. At channel 0.2, PS showcases a value of 205.7, surpassing ES at 194.3. At channel 0.8, PS scores 222.6, whilst ES [22], achieves 218.4. Even at channel 1, PS maintains its lead with 199.4. These results highlight PS as the best performer in terms of signal strength across the 9 channels, especially for ITR applications.

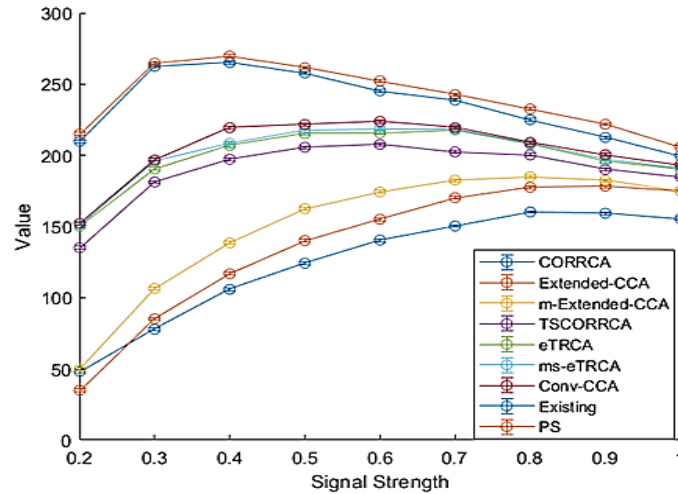


Figure 4. ITR graph of 9 channels for Benchmark dataset comparison

In Figure 5 the analysis of performance across 64 channels for ITR. PS consistently exhibits the highest signal strength values in all channels, signifying its strong performance. At channel 0.2, PS impressively scores 215, surpassing existing at 209.8. At channel 0.7, PS scores 242.6, and ES [22] achieves 238.75. Even at channel 1, PS maintains its lead with 205.8. These results underscore PS as the best performer in terms of signal strength across the 64 channels, particularly for ITR applications.

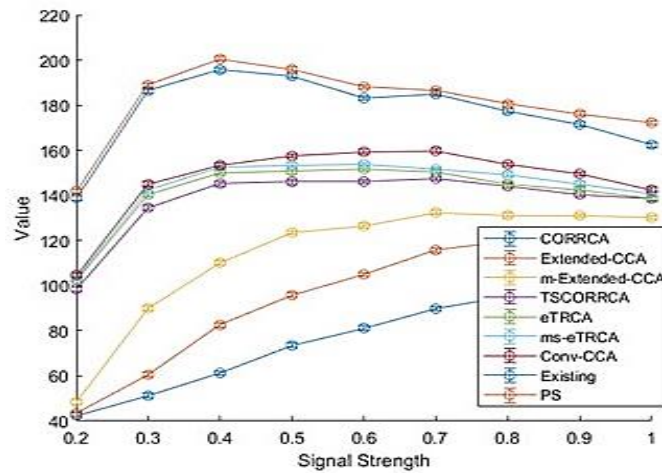


Figure 5. ITR graph of 64 channels for BETA dataset comparison

3.2. Comparative analysis

The comparative analysis is shown below for the Benchmark dataset. The improvisation of accuracy comparison for 9 channels and 64 channels is shown in Table 1. This shows the improvisation of the PS made over the ES, wherein the PS shows greater improvement in comparison with the ES.

3.2.1. Benchmark dataset

The comparative analysis is shown below for the Benchmark dataset. Wherein the improvisation of accuracy comparison for 9 channels, and 64 channels is shown below. This shows the improvisation of the PS made over the ES, wherein the PS shows greater improvement in comparison with the ES. The comparative analysis is shown below for the Benchmark dataset. The improvisation for ITR comparison for 9 channels and 64 channels as shown in Table 2. This shows the improvisation of the PS made over the ES, wherein the PS shows greater improvement in comparison with the ES.

Table 1. Accuracy comparison on Benchmark dataset

9-channel improvisation	64-channel improvisation
4.31	3.60
2.86	3.67
4.25	4.94
2.02	2.14
3.39	3.29
2.30	2.34
2.80	2.53
2.31	2.08
2.71	2.35

Table 2. ITR comparison on Benchmark dataset

9-channel improvisation ITR	64-channel improvisation ITR
5.87	2.62
2.17	0.84
1.14	1.79
0.88	1.43
0.70	2.89
2.23	1.60
1.92	3.33
1.48	4.38
2.05	3.06

4. CONCLUSION

In conclusion, the proposed methodology for SSVEP-based BCIs seeks to overcome the challenges in BCI adoption by streamlining calibration, enhancing ITRs, and simplifying user training. The research introduces invariant templates for SSVEP-based BCIs to improve detection accuracy amidst user response variations. The methodology encompasses critical stages, from data pre-processing and spatial filter design to testing, SSVEP detection, and sub-band decomposition. By optimizing these processes and employing spatial filters, this work aims to make SSVEP-based BCIs more user-friendly and accessible, ultimately empowering individuals with advanced communication and control capabilities, thereby enhancing their quality of life across applications like assistive technology and healthcare.

ACKNOWLEDGEMENT

I would like to express our sincere gratitude to all those who have supported and contributed to this research project. Primarily, I extend our heartfelt thanks to our guide for his unwavering guidance, invaluable insights, and encouragement throughout the research process. No funding is raised for this research.

REFERENCES

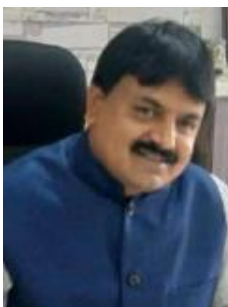
- [1] R. Zhang, G. Dong, M. Li, Z. Tang, X. Chen, and H. Cui, "A calibration-free hybrid BCI speller system based on high-frequency SSVEP and sEMG," *IEEE Transactions on Neural Systems and Rehabilitation Engineering*, vol. 31, pp. 3492–3500, 2023, doi: 10.1109/TNSRE.2023.3308779.
- [2] L. Cao *et al.*, "A novel real-time multi-phase BCI speller based on sliding control paradigm of SSVEP," *IEEE Access*, vol. 7, pp. 133974–133981, 2019, doi: 10.1109/ACCESS.2019.2941642.
- [3] K. Won, M. Kwon, S. Jang, M. Ahn, and S. C. Jun, "P300 speller performance predictor based on RSVP multi-feature," *Frontiers in Human Neuroscience*, vol. 13, Jul. 2019, doi: 10.3389/fnhum.2019.00261.
- [4] Z. Gu, Z. Chen, J. Zhang, X. Zhang, and Z. L. Yu, "An online interactive paradigm for P300 brain-computer interface speller," *IEEE Transactions on Neural Systems and Rehabilitation Engineering*, vol. 27, no. 2, pp. 152–161, Feb. 2019, doi: 10.1109/TNSRE.2019.2892967.
- [5] S. Duraisamy and R. M. Reddy, "Stimulus paradigm for an asynchronous concurrent SSVEP and EOG based BCI speller system," *IEEE Access*, vol. 9, pp. 127484–127495, 2021, doi: 10.1109/ACCESS.2021.3112257.
- [6] J. J. Podmore, T. P. Breckon, N. K. N. Aznan, and J. D. Connolly, "On the relative contribution of deep convolutional neural networks for SSVEP-based bio-signal decoding in BCI speller applications," *IEEE Transactions on Neural Systems and Rehabilitation Engineering*, vol. 27, no. 4, pp. 611–618, Apr. 2019, doi: 10.1109/TNSRE.2019.2904791.
- [7] T. H. Nguyen and W. Y. Chung, "A single-channel SSVEP-based BCI speller using deep learning," *IEEE Access*, vol. 7, pp. 1752–1763, 2019, doi: 10.1109/ACCESS.2018.2886759.
- [8] S. N. Aghili and A. Erfanian, "A P300-based speller design using a MINMAX riemannian geometry scheme and convolutional neural network," *IEEE Access*, vol. 11, pp. 98633–98652, 2023, doi: 10.1109/ACCESS.2023.3313260.
- [9] G. Ma, J. Kang, D. E. Thompson, and J. E. Huggins, "BCI-utility metric for asynchronous P300 brain-computer interface systems," *IEEE Transactions on Neural Systems and Rehabilitation Engineering*, vol. 31, pp. 3968–3977, 2023, doi: 10.1109/TNSRE.2023.3322125.
- [10] P. Pujar, A. Kumar, and V. Kumar, "Plant leaf detection through machine learning based image classification approach," *IAES International Journal of Artificial Intelligence*, vol. 13, no. 1, pp. 1139–1148, Mar. 2024, doi: 10.11591/ijai.v13.i1.pp1139-1148.
- [11] S. H. Sreedhara, V. Kumar, and S. Salma, "Efficient big data clustering using adhoc fuzzy C means and auto-encoder CNN," in *Lecture Notes in Networks and Systems*, vol. 563, Springer Nature Singapore, 2023, pp. 353–368.
- [12] K. Lin, S. Gao, and X. Gao, "Boosting the information transfer rate of an SSVEP-BCI system using maximal-phase-locking value and minimal-distance spatial filter banks," *Tsinghua Science and Technology*, vol. 24, no. 3, pp. 262–270, Jun. 2019, doi: 10.26599/TST.2018.9010010.
- [13] Z. Wang, C. Chen, J. Li, F. Wan, Y. Sun, and H. Wang, "ST-CapsNet: linking spatial and temporal attention with capsule network for P300 detection improvement," *IEEE Transactions on Neural Systems and Rehabilitation Engineering*, vol. 31, pp. 991–1000, 2023, doi: 10.1109/TNSRE.2023.3237319.
- [14] M. Nakanishi, Y. Te Wang, C. S. Wei, K. J. Chiang, and T. P. Jung, "Facilitating calibration in high-speed BCI spellers via leveraging cross-device shared latent responses," *IEEE Transactions on Biomedical Engineering*, vol. 67, no. 4, pp. 1105–1113, Apr. 2020, doi: 10.1109/TBME.2019.2929745.
- [15] R. Ma, T. Yu, X. Zhong, Z. L. Yu, Y. Li, and Z. Gu, "Capsule network for ERP detection in brain-computer interface," *IEEE Transactions on Neural Systems and Rehabilitation Engineering*, vol. 29, pp. 718–730, 2021, doi: 10.1109/TNSRE.2021.3070327.

- [16] M. Nakanishi, Y. Wang, X. Chen, Y. Te Wang, X. Gao, and T. P. Jung, "Enhancing detection of SSVEPs for a high-speed brain speller using task-related component analysis," *IEEE Transactions on Biomedical Engineering*, vol. 65, no. 1, pp. 104–112, Jan. 2018, doi: 10.1109/TBME.2017.2694818.
- [17] M. A. Khan, R. Das, H. K. Iversen, and S. Puthusserypady, "Review on motor imagery based BCI systems for upper limb post-stroke neurorehabilitation: From designing to application," *Computers in Biology and Medicine*, vol. 123, p. 103843, Aug. 2020, doi: 10.1016/j.compbiomed.2020.103843.
- [18] S. Le Bars, S. Chokron, R. Balp, K. Douibi, and F. Waszak, "Theoretical perspective on an ideomotor brain-computer interface: toward a naturalistic and non-invasive brain-computer interface paradigm based on action-effect representation," *Frontiers in Human Neuroscience*, vol. 15, Oct. 2021, doi: 10.3389/fnhum.2021.732764.
- [19] M. Xu, J. Han, Y. Wang, and D. Ming, "Optimizing visual comfort and classification accuracy for a hybrid P300-SSVEP brain-computer interface," in *International IEEE/EMBS Conference on Neural Engineering, NER*, May 2017, pp. 363–366, doi: 10.1109/NER.2017.8008365.
- [20] X. Li *et al.*, "A hybrid steady-state visual evoked response-based brain-computer interface with MEG and EEG," *Expert Systems with Applications*, vol. 223, p. 119736, Aug. 2023, doi: 10.1016/j.eswa.2023.119736.
- [21] A. Liu, Q. Liu, X. Zhang, X. Chen, and X. Chen, "Muscle artifact removal toward mobile SSVEP-based BCI: a comparative study," *IEEE Transactions on Instrumentation and Measurement*, vol. 70, pp. 1–12, 2021, doi: 10.1109/TIM.2021.3085944.
- [22] H. Y. Zhang, C. E. Stevenson, T. P. Jung, and L. W. Ko, "Stress-induced effects in resting EEG spectra predict the performance of SSVEP-based BCI," *IEEE Transactions on Neural Systems and Rehabilitation Engineering*, vol. 28, no. 8, pp. 1771–1780, Aug. 2020, doi: 10.1109/TNSRE.2020.3005771.
- [23] J. Lin, L. Liang, X. Han, C. Yang, X. Chen, and X. Gao, "Cross-target transfer algorithm based on the volterra model of SSVEP-BCI," *Tsinghua Science and Technology*, vol. 26, no. 4, pp. 505–522, Aug. 2021, doi: 10.26599/TST.2020.9010015.
- [24] Y. Wang, X. Chen, X. Gao, and S. Gao, "A benchmark dataset for SSVEP-based brain-computer interfaces," *IEEE Transactions on Neural Systems and Rehabilitation Engineering*, vol. 25, no. 10, pp. 1746–1752, Oct. 2017, doi: 10.1109/TNSRE.2016.2627556.
- [25] O. B. Guney, M. Oblokulov, and H. Ozkan, "A deep neural network for SSVEP-based brain-computer interfaces," *IEEE Transactions on Biomedical Engineering*, vol. 69, no. 2, pp. 932–944, Feb. 2022, doi: 10.1109/TBME.2021.3110440.

BIOGRAPHIES OF AUTHORS



Mrs. Manjula Krishnappa    is currently working as Assistant Professor in ECE department at SJC Institute of Technology, Chickballapur with 10 years of teaching experience and research scholar at BGSIT, Mandya. She guided 20+ UG projects, with 21 National journals and 13 international journals which includes 4 Scopus indexed journals. Five KSCST projects are sanctioned, filed 1 patent and her areas of interests are biomedical signal processing, VLSI design, and MEMS. She can be contacted at this email: manjula22k@rediffmail.com.



Dr. Madaveeranahally B. Anandaraju    is currently working as professor and head in the department of ECE, BGSIT, Mandya. He is having 22 years of teaching experience. Obtained his Ph.D. degree from university of Mysore. He has guided 40+ UG and PG projects and guiding 3 Ph.D. scholars. He has published more than 30 papers in reputed international journals. He has 1 patent grant; 3 more patents are filed and one VGST project is sanctioned. He has served at various academic levels of the institution. His areas of interests are biomedical signal processing, neural networks, and power electronics. He can be contacted at this email: mbanandraj@yahoo.com.